Reprint

A Journal of the Gesellschaft Deutscher Chemiker

Angewandte Chemie

International Edition

Bioorganic Chemistry

Irreversible Inhibition of Metallo-β-lactamase (IMP-1) by 3-(3-Mercapto-propionylsulfanyl)propionic Acid Pentafluorophenyl Ester

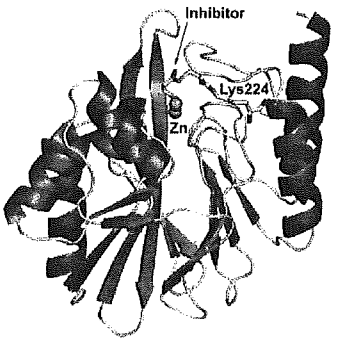

Resistance is futile: Pathogenic bacteria that produce metallo-β-lactamases are recognized as a serious threat because of their resistance to antibiotics. The title compound has now been shown to be an irreversible inhibitor for a metallo-β-lactamase (IMP-1). The X-ray crystallographic structure (see picture) has revealed that the inhibitor binds to IMP-1 with formation of a covalent amide bond with the amino group (N^{ζ}) of Lys 224.

H. Kurosaki,* Y. Yamaguchi, T. Higashi, K. Soga, S. Matsueda, H. Yumoto, S. Misumi, Y. Yamagata, Y. Arakawa, M. Goto

Keywords: bioorganic chemistry · inhibitors · lactams · metalloenzymes · structure elucidation

2005 – 44/25

WILEY-VCH

Bioorganic Chemistry

Irreversible Inhibition of Metallo-β-lactamase (IMP-1) by 3-(3-Mercaptopropionylsulfanyl)-propionic Acid Pentafluorophenyl Ester**

Hiromasa Kurosaki, Yoshihiro Yamaguchi, Toshihiro Higashi, Kimitaka Soga, Satoshi Matsueda, Haruka Yumoto, Shogo Misumi, Yuriko Yamagata, Yoshichika Arakawa, and Masafumi Goto*

Pathogenic bacteria that produce metallo-β-lactamases (MBLs) are emerging as a new challenge to the medical community. These enzymes catalyze the hydrolysis of a wide spectrum of β-lactams, including carbapenems such as imipenem, some of which are coded in transferable plasmids.[1,2] Among the currently known MBLs, IMP-1, a member of subclass B1, which is encoded by the bla_{IMP} gene included in the integron structure,[2,3] rapidly spreads by facile horizontal gene transfer to other bacteria.[4] Moreover, many of the currently used serine β-lactamase inhibitors such as clavulanic acid, sulbactam, and tazobactam are ineffective against MBLs. Thus, the development of inhibitors of MBLs is important for the continuing application of such widely prescribed β-lactam antibiotics. Several such inhibitors have been reported to date;[5–11] for example, Payne et al. demonstrated[6] that mercaptoacetic acid, a hydrolysis product of mercaptoacetic acid thiol esters that are hydrolyzed by MBLs (β-lactamase II, CfiA, and CphA), binds irreversibly to the enzyme through formation of a disulfide bond with the active site cysteine residue under aerobic conditions, as evidenced

[*] Prof. Dr. H. Kurosaki, Y. Yamaguchi, T. Higashi, K. Soga, S. Matsueda, H. Yumoto, Prof. Dr. M. Goto
Department of Structure-Function Physical Chemistry
Graduate School of Pharmaceutical Sciences
Kumamoto University
Oe-honmachi 5-1, Kumamoto 862-0973 (Japan)
Fax: (+81) 96-371-4314
E-mail: ayasaya@gpo.kumamoto-u.ac.jp
Prof. Dr. S. Misumi
Department of Pharmaceutical Biochemistry
Graduate School of Pharmaceutical Sciences
Kumamoto University
Oe-honmachi 5-1, Kumamoto 862-0973 (Japan)
Prof. Dr. Y. Yamagata
Department of Structural Biology
Graduate School of Pharmaceutical Sciences
Kumamoto University
Oe-honmachi 5-1, Kumamoto 862-0973 (Japan)
Prof. Dr. MD. Y. Arakawa
Department of Bacterial Pathogenesis and Infection Control
National Institute of Infectious Diseases
4-7-1 Gakuen, Musashi-Murayama, Tokyo 208-0011 (Japan)

[**] This work was supported by H15-Shinkou-9 from the Ministry of Health Labor and Welfare of Japan and by a Grant-in-Aid for Scientific Research (B) (No. 16390017) from the Japan Society for the Promotion of Science.

Supporting information for this article is available on the WWW under http://www.angewandte.org or from the author.

 DOI: 10.1002/anie.200500835

by both tryptic digestion and electrospray mass spectrometry studies.

Our ultimate goal was to develop an irreversible inhibitor of IMP-1. We report here on the design and inhibition properties of three-dimensional structure-based irreversible inhibitors of IMP-1, **1** and **2**, and the crystal structure of a covalently bound complex formed between the hydrolysis product of **2** and IMP-1.

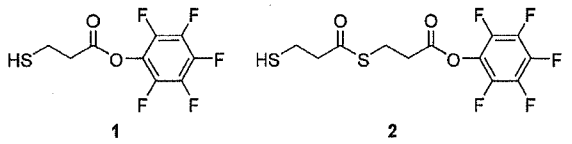

1 **2**

The strategy for the irreversible inhibition of IMP-1 is shown in Scheme 1: The thiol group in **2** coordinates to one or

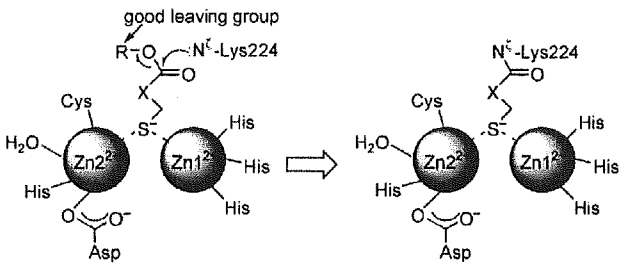

Scheme 1. Strategy for the irreversible inhibition of thiol compounds with a good leaving group.

two Zn^{II} ion(s) in the active site as an anchor. Lys224 (following BBL numbering[12]) is conserved in almost all MBLs of subclass B1. In the first IMP-1 structure reported (PDB code 1DD6),[7] Lys224 is located at a distance of about 6 Å from the two Zn^{II} ions. Lys224 is thought to be important for substrate binding[6,13] and may attack an activated ester, thus forming a covalently bound inhibitor–enzyme adduct that irreversibly inhibits the enzyme. At this point, water molecules, from the solvation shell surrounding Lys224, may act as acceptors of H^+ ions from the positively charged N^{ζ} group of Lys224.

The coupling reaction of one equivalent of 3-mercaptopropionic acid (MPA) and 1-hydroxy-1*H*-benzotriazole (HOBt) with pentafluorophenol in the presence of one equivalent of *N,N'*-dicyclohexylcarbodiimide (DCC) in ethyl acetate at 0 °C afforded **1**, a synthetic intermediate of **2**, in 15% yield (see Supporting Information). The desired inhibitor **2** was prepared in 45% yield by treating **1** with MPA in the presence of DCC in ethyl acetate at 0 °C (see Supporting Information).

The time-dependent inactivation of IMP-1 by **1** and **2** was determined by incubating various amounts of inhibitor with 10 nM IMP-1 in 50 mM tris-HCl/0.5 M NaCl buffer (pH 7.4, tris = tris(hydroxymethyl)aminomethane) at 15 °C (see Supporting Information). The inactivation of IMP-1 by **1** and **2** was both time and concentration dependent. Plots of the natural logarithm of the residual activity against incubation time were linear, thus suggesting that the observed rate of inactivation follows pseudo-first-order kinetics (Figure 1a and b). The double reciprocal plots of these slopes (k_{obs}) versus concentration of **1** and **2** gave straight lines (Figure 1c

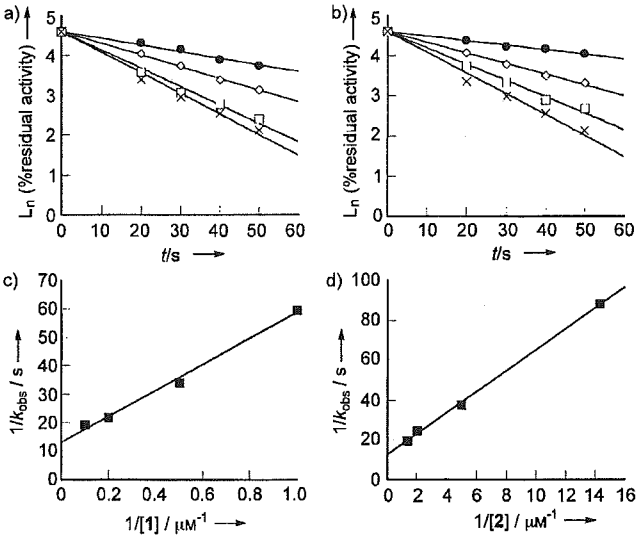

Figure 1. Time- and concentration-dependent inactivation of IMP-1 by **1** (a) and **2** (b) in 50 mM tris-HCl/0.5 M NaCl buffer (pH 7.4) at 15 °C. Inhibition concentrations: ●: 1 μM; ◇: 2 μM; □: 5 μM; and ×: 10 μM for **1**, and ●: 0.07 μM; ◇: 0.2 μM; □: 0.5 μM; and ×: 0.75 μM for **2**. Each point shown represents the mean of three experiments. Double reciprocal plots of k_{obs} versus concentration of **1** (c) and **2** (d).

and d). The regression line did not pass through the origin, but intercepted the positive *y*-axis, thus indicating the initial formation of a dissociable complex between IMP-1 and inhibitor before inactivation.[14] The k_{inact} and K_i values were calculated from these plots to be 0.076 ± 0.002 s^{-1} and 3.452 ± 0.030 μM for **1** and 0.080 ± 0.002 s^{-1} and 0.423 ± 0.013 μM for **2**. These results show that the second-order rate constant for inactivation (k_{inact}/K_i) with **2** increases by about ninefold over that with **1**.

To determine whether **1** or **2** inhibits IMP-1 irreversibly, 10 μM IMP-1 was incubated with 1 mM **1** or **2** at 0 °C for various periods of time (0–2 h) and the mixtures were then filtered through gel (Sephadex G-25) to separate the protein from the excess inhibitor (see Supporting Information). The activity of the resulting protein was measured using nitrocefin as the substrate. The control, without inhibitor, shows no loss of activity of IMP-1 after filtration through the gel. On the other hand, the inactivation of IMP-1 by **1** and **2** resulted in a nearly 100% inhibition, clearly showing that both inhibitors inhibited IMP-1 very rapidly and irreversibly. Furthermore, the irreversibility of the binding of **1** and **2** was also confirmed by dialysis at 4 °C for 16 h (see Supporting Information): in neither of these cases was any activity recovered, thus verifying that **1** and **2** are irreversible inhibitors.

After the incubation of 100 μM **2** with 10 μM IMP-1 for 30 minutes and gel filtration, the sample was analyzed by MALDI-TOF mass spectrometry (see Supporting Information). The MALDI-TOF mass spectrum of the intact IMP-1

showed the parent signal at *m/z* 25113.2 while that treated with **2** showed a peak at *m/z* 25290.1 (see Supporting Information). The increase in mass of *m/z* 176.9 corresponds to the mass of $SCH_2CH_2COSCH_2CH_2CO$ (this unit is denoted **2**-P), which indicates that this moiety of **2** is covalently attached to IMP-1 in a ratio of 1:1.

To identify the site of amino acid attachment and to determine the three-dimensional structure, crystals of IMP-1 treated with **2** were prepared by the hanging-drop method and the molecular structure was determined (see Supporting Information). The structure of the inhibitor bound IMP-1 (**2**-P/IMP-1) at a resolution of 2.63 Å was refined to an *R*-factor value of 22.8% and an R_{free} value of 24.3% using 2.63- to 44.7-Å data.[15] There are two **2**-P/IMP-1 molecules, A and B, in the asymmetric unit. The two molecules are almost identical with a root-mean-square deviation of 0.31 Å when all C^{α} atoms between A and B are superimposed. The overall structure of each molecule adopts a αβ/βα sandwich structure as found in the native enzyme, the three-dimensional structure of which was not greatly perturbed by the inhibitor. The overall structure of molecule A is shown in Figure 2a.

The thiolate group in **2**-P bridges between the two Zn^{II} ions in the active site (distances Zn1···inhibitor(S), 2.2/2.2; Zn2···inhibitor(S), 2.3/2.5 Å in molecules A/B; Figure 2b). The geometry around Zn2 is changed from a trigonal bypyramid in the native structure to a distorted tetrahedral structure, as previously reported by Concha et al.[7] (angles (Asp120)$O^{\delta 2}$-Zn2-Cys221(S^{γ}), 101/101°; (Asp120)$O^{\delta 2}$-Zn2-His263($N^{\varepsilon 2}$), 99/104°; Asp120 $O^{\delta 2}$-Zn2-inhibitor(S), 122/112°; (Cys221)S^{γ}-Zn2-His263($N^{\varepsilon 2}$), 109/116°; (Cys221)S^{γ}-Zn2-inhibitor(S), 107/113°; (His263)$N^{\varepsilon 2}$-Zn2-inhibitor(S), 117/111° in molecules A/B.

The $2|F_o|-|F_c|$ electron density map clearly indicates the formation of a covalent amide bond between the ester and side chain N^{ζ} atom of Lys224 with the concomitant displacement of the pentafluorophenolate group, which is not seen in the electron density.

The carbonyl oxygen atom of the amide group formed between the inhibitor and IMP-1 forms a hydrogen bond with the main-chain nitrogen atom of Asn233 (ca. 3.1/3.3 Å in molecules A/B) while the carbonyl oxygen atom of the thioester group of the inhibitor is hydrogen bonded to the side chain nitrogen atom of Asn233 (ca. 3.0/3.5 Å in molecules A/B).

In summary, the synthesis of a covalent, irreversible inhibitor **2** of IMP-1 is described. An X-ray crystal structure of the inhibitor covalently bound to IMP-1 confirmed this strategy. These findings shed further light on the design of inhibitors based on the three-dimensional structure of MBLs related to IMP-1.

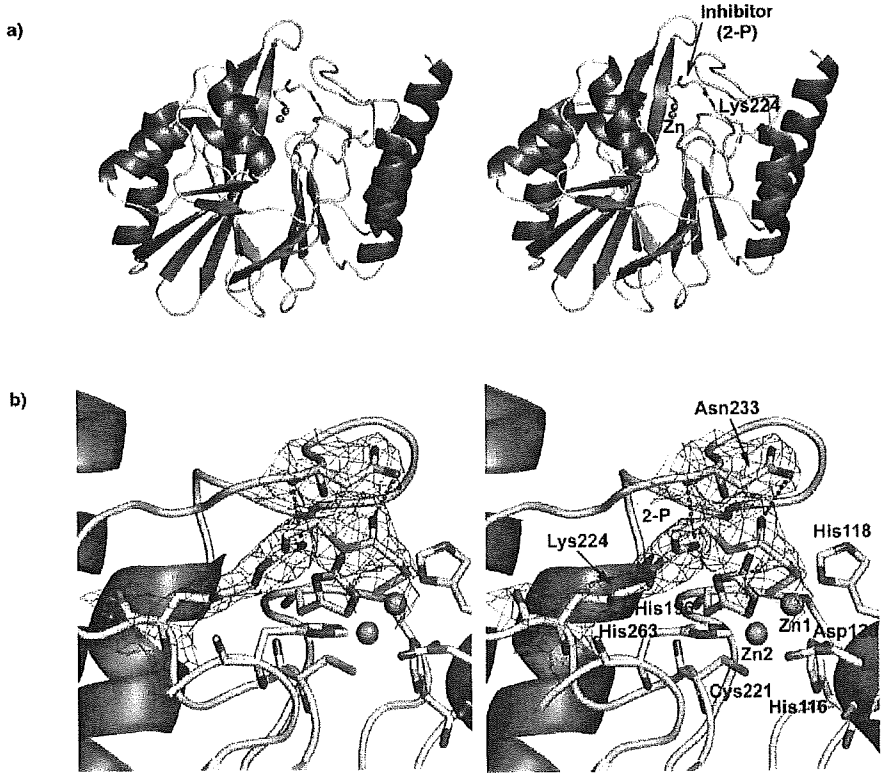

Figure 2. a) The overall structure of IMP-1 complexed with 2-P. α-Helices, β-strands, and loops are shown in red, green, and yellow, respectively. Zn^{2+} ions are represented as orange spheres. The inhibitor and Lys224 are displayed as sticks (C, N, O, and S atoms colored gray, blue, red, and green, respectively). b) The crystal structure of IMP-1 modified by **2**-P. The electron density of Asn233 as well as Lys224 and its covalently attached inhibitor molecule is shown countoured at 1.0σ in a $2|F_o|-|F_c|$ map. Hydrogen bonds are indicated by blue dashed lines.

Received: March 7, 2005
Published online: May 13, 2005

Keywords: bioorganic chemistry · inhibitors · lactams · metalloenzymes · structure elucidation

[1] Y. Arakawa, M. Murakami, K. Suzuki, H. Ito, R. Wacharotayankun, S. Ohsuka, N. Kato, M. Ohta, *Antimicrob. Agents Chemother.* **1995**, *39*, 1612–1615.
[2] M. L. Riccio, N. Franceschini, L. Boschi, B. Caravelli, G. Cornaglia, R. Fontana, G. Amicosante, G. M. Rossolini, *Antimicrob. Agents Chemother.* **2000**, *44*, 1229–1235.
[3] N. Laraki, M. Galleni, I. Thamm, M. L. Riccio, G. Amicosante, J. M. Frère, G. M. Rossolini, *Antimicrob. Agents Chemother.* **1999**, *43*, 890–901.
[4] D. M. Livermore, N. Woodford, *Curr. Opin. Microbiol.* **2000**, *3*, 489–495.
[5] M. Goto, T. Takahashi, F. Yamashita, A. Koreeda, H. Mori, M. Ohta, Y. Arakawa, *Biol. Pharm. Bull.* **1997**, *20*, 1136–1140.
[6] D. J. Payne, J. H. Bateson, B. C. Gasson, D. Proctor, T. Khushi, T. H. Farmer, D. A. Tolson, D. Bell, P. W. Skett, A. C. Marshall, R. Reid, L. Ghosez, Y. Combret,

J. Marchand-Brynaert, *Antimicrob. Agents Chemother.* **1997**, *41*, 135–140.
[7] N. O. Concha, C. A. Janson, P. Rowling, S. Pearson, C. A. Cheever, B. P. Clarke, C. Lewis, M. Galleni, J. M. Frère, D. J. Payne, J. H. Bateson, S. S. Abdel-Meguid, *Biochemistry* **2000**, *39*, 4288–4298.
[8] J. H. Toney, G. G. Hammond, P. M. Fitzgerald, N. Sharma, J. M. Balkovec, G. P. Rouen, S. H. Olson, M. L. Hammond, M. L. Greenlee, Y. D. Gao, *J. Biol. Chem.* **2001**, *276*, 31913–31918.
[9] S. Bounaga, M. Galleni, A. P. Laws, M. I. Page, *Bioorg. Med. Chem.* **2001**, *9*, 503–510.
[10] S. Siemann, D. P. Evanoff, L. Marrone, A. J. Clarke, T. Viswanatha, G. I. Dmitrienko, *Antimicrob. Agents Chemother.* **2002**, *46*, 2450–2457.
[11] I. García-Sáez, J. Hopkins, C. Papamicael, N. Franceschini, G. Amicosante, G. M. Rossolini, M. Galleni, J. M. Frère, O. Dideberg, *J. Biol. Chem.* **2003**, *278*, 23868–23873.
[12] M. Galleni, J. Lamotte-Brasseur, G. M. Rossolini, J. Spencer, O. Dideberg, J. M. Frère, *Antimicrob. Agents Chemother.* **2001**, *45*, 660–663.
[13] S. Haruta, E. T. Yamamoto, Y. Eriguchi, T. Sawai, *FEMS Microbiol. Lett.* **2001**, *197*, 85–89.
[14] R. Kitz, I. B. Wilson, *J. Biol. Chem.* **1962**, *237*, 3245–3249.
[15] The X-ray coordinates for the **2**-P/IMP-1 complex have been deposited in the Protein Data Bank under the code number: 1VGN.

蛋白質核酸酵素
PNE
PROTEIN, NUCLEIC ACID AND ENZYME

別刷

「蛋白質 核酸 酵素」編集部
共立出版株式会社
〒112-8700　東京都文京区小日向 4-6-19
Tel.03-3947-2515　FAX 03-3944-8182
E-mail：pne@kyoritsu-pub.co.jp
http://www.kyoritsu-pub.co.jp/

特集

病原細菌と外界を結ぶチャネル：薬剤排出ポンプと病原因子分泌装置

細菌のマルチコンポーネント型RND異物排出システム群の機能

抗菌薬耐性研究から病原因子産生制御機構研究へのプロローグ

後藤直正

細菌の染色体上にコードされた排出システムの研究は，化学療法史上かつてない広域交差耐性をもたらす機構として，臨床上重要な病原性細菌を中心に行なわれてきたが，同時に，この排出システムの生理的機能は何かが問われつづけてきた．現在，それに対する答えが得られつつある．そのひとつが，細菌の生育環境に存在する細胞障害性異物からの自己防御であり，もうひとつは，細菌間のコミュニケーションに機能し病原性因子産生の引き金となるオートインデューサー化合物の排出である．排出システムの研究によって，抗菌薬耐性と病原性という，本来は結びつかなかった機構のつながりがみえるようになってきた．

Key words 排出システム　抗菌薬耐性　病原因子　緑膿菌

はじめに

細菌のみならず，多くの生物種のゲノム配列が解明されるにつれ，トランスポーター(transporter；輸送担体)の遺伝子がゲノム上で大きな割合を占めることが明らかにされてきた．細胞膜により自己と環境を隔てる生物にとって，変化する環境から種々の栄養物を摂取したり，逆に細胞内代謝産物を分泌したりするためには，複雑に機能分化したトランスポーターが必要なのであろう．トランスポーターは，細胞外から細胞内へ細胞膜をこえて輸送するものと，細胞内から細胞外へ輸送するものとに分けることができる．本稿で対象とするⅠ型分泌機構[1]は，細胞内から細胞外へ輸送するトランスポーターの一種である．さらに，Ⅰ型分泌機構は多剤排出ポンプ[→今月のKey Words (p.5)]として，細胞内代謝産物や細胞外から透過進入した細胞障害性分子，いわゆる異物の細胞外への輸送に機能している．Ⅰ型分泌機構が細菌内に透過した抗菌薬や消毒薬などを排出し，それらに対する抵抗性(耐性)を付与することから，これまでは抗菌薬や消毒薬耐性機構の面から多くの研究がなされてきた．そこで，抗菌薬排出に働くシステムを抗菌薬排出システムとよんできたが，これらは抗菌薬に限るものではなく，消毒薬，抗菌性色素，有機溶媒，重金属の排出にも働くものがほとんどである．さらには，異物に対する耐性のみならず，細菌の病原性発揮にも重要な役割を果たしているものがあり，排出システムの生理的機能が明らかになりつつある．

細菌の排出システムは，駆動のためのエネルギー種，排出蛋白質の分子サイズ，アミノ酸1次配列におけるホモロジーや高次構造をもとに，ATP加水分解によって駆動するATP-binding cassette(ABC)スーパーファミリー，細胞質膜内外に形成されたプロトン勾配を駆動力とするsmall multidrug resistance(SMR)ファミリー，major facilitator superfamily(MFS)，およびresistance-nodulation-cell division(RND)ファミリー，さらには細胞質膜の内外に形成されたナトリウムイオン勾配によって駆動するmultidrug and toxic compound extrusion(MATE)ファミリーの5つのファミリーに分類されている(図1)[2]．これらのファミリーのそれぞれには，1種類の排出蛋白質コンポーネントのみで機能するモノコンポーネント型と，排出蛋白質の機能を助けるコンポー

Naomasa Gotoh，京都薬科大学 微生物学教室　E-mail：ngotoh@mb.kyoto-phu.ac.jp

Bacterial RND-type multicomponent efflux systems：The efflux systems involve to production of pathogenic factors as well as resistance to antimicrobial agents

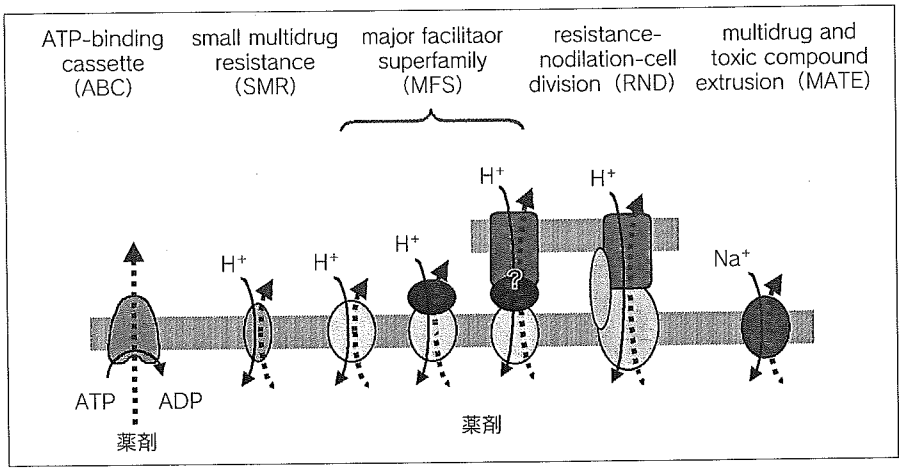

図 1　細菌の排出システム
細菌の排出システムは，排出のために必要なエネルギー源(ATP 加水分解，プロトン勾配，ナトリウム勾配)と，排出蛋白質の分子サイズ，アミノ酸配列のホモロジーおよび高次構造などから，少なくとも 5 つのファミリーに分けることができる．また，これらは，1 種類の排出蛋白質だけで機能するモノコンポーネント型と，排出蛋白質とそれと共同して働く複数のコンポーネントからなるマルチコンポーネント型とに分けられる．

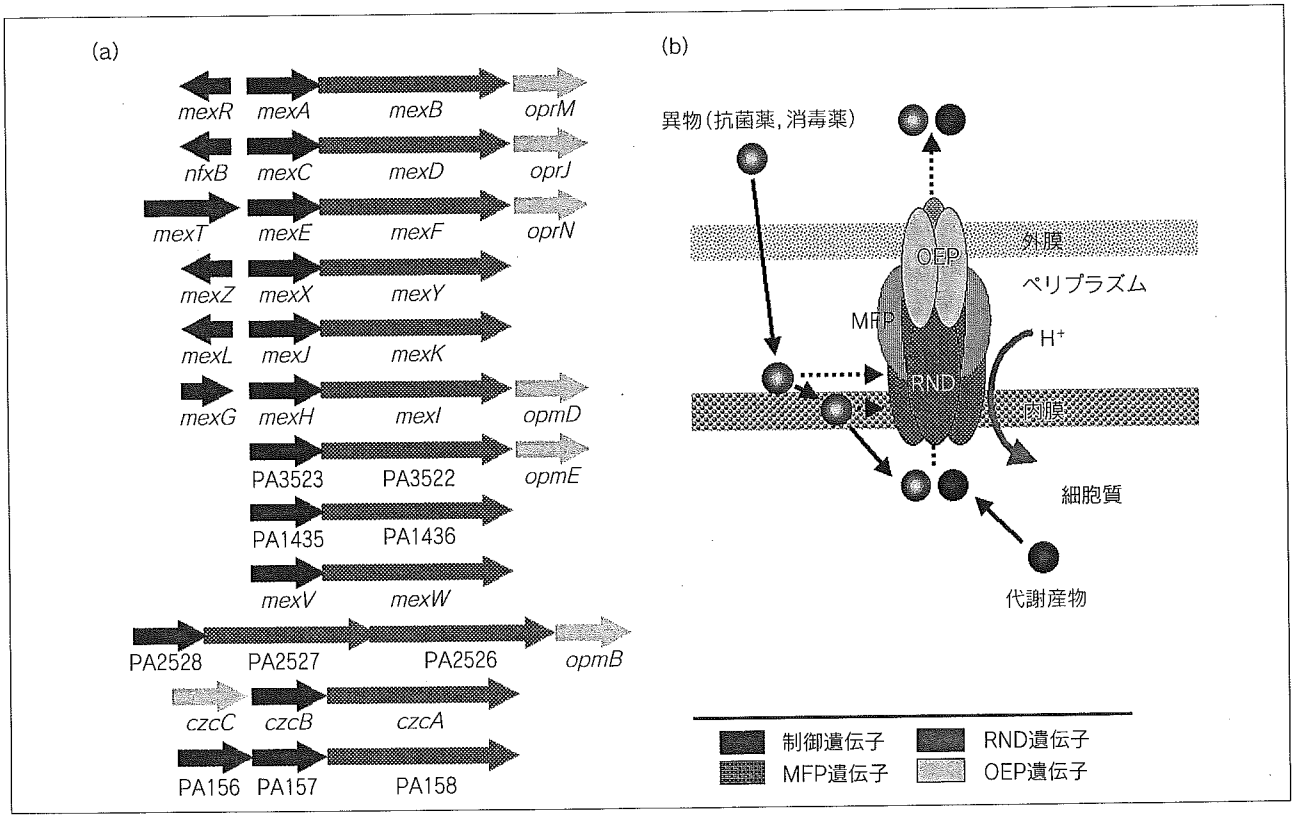

図 2　マルチコンポーネント型 RND 排出システム
緑膿菌染色体にコードされたマルチコンポーネント型 RND 排出システムのオペロン群(a)と，それらの遺伝子の発現により形成されるマルチコンポーネント型排出システム(b)．

ネントとの共同作業によって機能するマルチコンポーネント型のものがある．

本稿では，緑膿菌（*Pseudomonas aeruginosa*）での研究成果を中心に，大腸菌（*Escherichia coli*），*Haemophilus influenzae*，淋菌(*Neissria gonorrhoeae*)などのグラム陰性菌での研究成果も加えて，マルチコンポーネント型 RND 多剤排出システムの多様性，抗菌薬耐性への関与，さらには病原性について稿を進める．種々の細菌での排出システムと抗菌薬耐性については，他の総説[3,4]を参照されたい．

I. マルチコンポーネント型異物排出システムの多様性と遺伝子構造

グラム陰性菌で研究成果が蓄積されたマルチコンポーネント型排出システムは，RNDファミリー排出蛋白質(RND efflux protein；RND)と外膜蛋白質(outer membrane efflux protein；OEP)，さらに，それらを結合する機能をもつペリプラズム蛋白質(membrane fusion protein；MFP)から形成されている(図2)．これらの排出システム遺伝子群はひとつの転写単位としてオペロンを形成しているが，OEP遺伝子と排出システムの制御遺伝子の存在様式により特徴的な差がみられる．

1. OEP遺伝子からみた排出システムオペロンの特徴

これらの排出システムは，基本的にはMFP遺伝子とRND遺伝子がひとつの転写単位としてオペロン構造を形成している．さらに，特定のOEP遺伝子がRND遺伝子の下流にコードされている場合とそうでない場合とがある．緑膿菌の染色体上には，これらの2種のオペロンが混在している[5]．前者のような排出システムオペロンは，緑膿菌以外では，*Pseudomonas putida*，*Burkholderia cepacia*，*Stenotrophomonas maltophilia*や淋菌などで発見されている[3]．

筆者らは，マルチコンポーネント型排出システムを構成する3種類のコンポーネントの機能解析のため，各コンポーネントを別の排出システムのコンポーネントと置き換えたキメラ排出システムを緑膿菌で発現させた[6,7]．その結果，OEPコンポーネントとRNDコンポーネントを置き換えたキメラ体で排出活性が観察されたこと，RNDコンポーネントの置き換えは基質認識を変化させるが，OEPコンポーネントの置き換えは基質認識には影響しないことを見いだし，RNDコンポーネントが基質認識に寄与すると結論した．しかし，緑膿菌染色体には排出システムオペロン上以外にも，OEPコンポーネントのホモログであるOprMファミリー外膜蛋白質が多種コードされている(http://cmdr.ubc.ca/bobh/；http://www.pseudomonas.com)．この意義を調べるため，OEP遺伝子をコードしない排出システム発現株(MexJ-MexK)に，OprMファミリー外膜蛋白質遺伝子をクローン化したプラスミドを導入し発現させたところ，MFPコンポーネントとRNDコンポーネントのペアが，生育環境に存在する異物種によって協同するOprMファミリー外膜蛋白質を選び，基質認識を変化させることを見いだした(筆者ら：投稿中)．これらのことは，緑膿菌は染色体にコードされた多くのマルチコンポーネント型排出システムの基質認識バリエーションに加えて，多種のOprMファミリー外膜蛋白質の使い分けによってさらにバリエーションを多様化していることを示唆している．緑膿菌と同じように，*P. putida*，*B. cepacia*や*S. maltophilia*の染色体上にも，多種のマルチコンポーネント型排出システムと多種の外膜蛋白質がコードされている．これらの細菌が基質認識バリエーションの高い機構をもつことが，高い異物代謝能と，土壌，水系，動物，植物などの多種の環境への適応能を付与した一因であると想像させる．

一方，大腸菌[8]や*H. influenzae*(http://www.tigr.org)の染色体にコードされたマルチコンポーネント型RND排出システムオペロンのすべてにはOEP遺伝子はコードされず，別の遺伝子にコードされる多機能な外膜蛋白質TolCがこのOEPコンポーネントの役割を果たしている．また，これらの菌種にはTolCの役割を代替するようなホモログが見いだされない．大腸菌や*H. influenzae*の場合，TolCの欠失は多くの排出システムの機能を消失させる[9]ことからも，これらの細菌がもつOEPコンポーネントはTolCに限られるようである．

2. 発現制御遺伝子からみた排出システムオペロンの特徴

排出システムオペロンのクローン化と大腸菌内での性状解析の例は多いが，もともとの細菌での発現を調べた例は意外と少なく，そのほとんどが緑膿菌で行なわれたものである．緑膿菌での研究から考えると，その多くは実験室条件では発現が抑制されていることが多い．この発現を抑制する制御遺伝子が排出システムオペロンの上流に逆向きに存在する場合がある．臨床や実験室で分離される排出システムの発現亢進によって抗菌薬耐性を獲得した株のほとんどは，この制御遺伝子に変異が起こり，その結果，排出システムの発現抑制が解除されたことによるものである．たとえば，緑膿菌の*nalB-mexA-mexB-oprM*オペロンでは，実験室の培養では*nalB*遺伝子産物による発現抑制によって*mexA-mexB-oprM*オペロンはわずかしか発現していないが，*nalB*遺伝子に変異が起こると高発現する[3](図3)．事実，抗菌薬耐性菌の多くにその変異が見いだされている．緑膿菌では，*nfxB*-

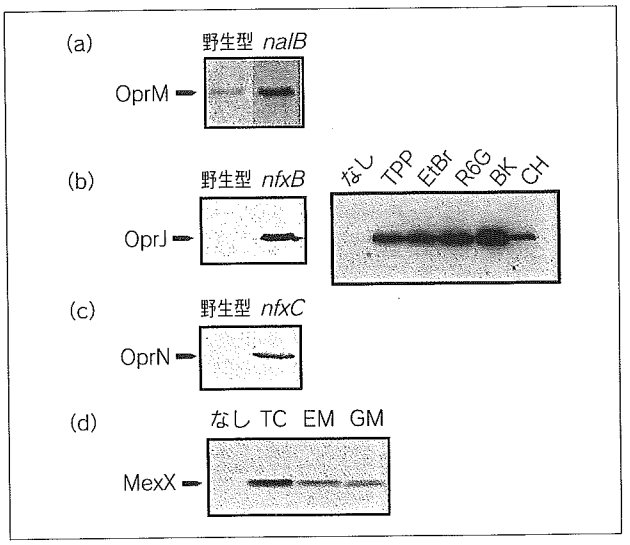

図 3　緑膿菌の代表的な排出システムの発現
排出システムのコンポーネントに対する特異抗体によるウェスタンブロット法によって，排出システムの発現を検出した．(a)抗 OprM モノクローナル抗体による検出．MexA-MexB-OprM システムは野生株でもわずかに発現しているが，*nalB* 遺伝子変異によって高発現する．(b)抗 OprJ モノクローナル抗体による検出．MexC-MexD-OprJ システムの発現は野生株では検出限界以下であるが，*nfxB* 遺伝子変異によって高発現する．一方，生育培地内の細胞障害性異物(TPP：トリフェニルリン酸，EtBr：エチジウムブロミド，R6G：ローダミン 6G，BK：塩化ベンザルコニウム，CH：クロロヘキシジン)の存在によっても発現する．(c)抗 OprN モノクローナル抗体による検出．MexE-MexF-OprN システムの発現は野生株では検出限界以下であるが，*nfxC* 変異によって高発現する．(d)抗 MexX ポリクローナル抗体による検出．MexX-MexY-OprJ システムの発現は野生株では検出限界以下であるが，生育培地内の抗菌薬(TC：テトラサイクリン，EM：エリスロマイシン，GM：ゲンタマイシン)の存在によって発現する．

mexC-mexD-oprJ オペロン[3]，*mexZ-mexX-mexY* オペロン[3]，*mexL-mexJ-mexK* オペロン[10]が，*nalB-mexA-mexB-oprM* オペロンと同じように発現を制御されていることが明らかにされてきたが，最近，*mexA-mexB-oprM* オペロンの高発現株を使った実験で，この発現は *nalB* 遺伝子のみならず，まったく別のオペロン PA3719-PA3720-PA3721(*nalC*)によっても制御されているという結果[11]が報告され，このオペロンは複雑な機構によって発現が制御されているようである．このように，制御遺伝子の変異によって排出システムの発現抑制が解除される例は，緑膿菌のみならず，ほかのグラム陰性菌でも報告されており，淋菌の *mtrC-mtrD-mtrE* オペロンでは，上流の制御遺伝子 *mtrR* の変異に加えて，*mtrR* 遺伝子と *mtrC* 遺伝子の遺伝子間領域に存在するオペレーター領域の変異によっても発現抑制が起こることが示されている[12]．

一方，緑膿菌の *mexT-mexE-mexF-oprN* オペロンでは，*mexT* 遺伝子が排出システムの本体をコードする *mexE-mexF-oprN* オペロンの発現を促進する遺伝子として働いている．しかし，実験室株ではこのオペロンの発現は観察されないこと，また，抗菌薬の選択によってもこのオペロンの高発現株が出現しない場合があることが知られてきた．高発現株が出現しない原因としては，緑膿菌の種々の実験室株では *mexT* 遺伝子に 8 塩基の挿入と点変異が起こり，これらの変異によって *mexT* 遺伝子が破壊されていることが Maseda らによって明らかにされた[13]．しかし，*mexT* 遺伝子以外にも制御遺伝子が存在することが予想されてきたが，現在でもその制御遺伝子は同定されていない．

もうひとつの発現制御のパターンは，排出システムオペロンの発現が，制御遺伝子の変異だけではなく，細菌の生育環境に存在する細胞障害性異物の存在や，増殖期に応じて発現する場合である．前者の例としては緑膿菌の *mexC-mexD-oprJ* オペロン[14]や *mexX-mexY* オペロン[15](図 3)が，後者の例としては緑膿菌の *mexG-mexH-mexI-opmD* オペロン[16]がある．発現誘導のメカニズムは現在のところわからないが，後者ではのちに述べる細菌間コミュニケーション機構が関与していることが示唆されている．

以上のように，排出システムオペロンの発現については制御遺伝子の変異による例が多く研究されてきた．しかし，制御遺伝子の有無にかかわらず，多くの排出システムオペロンで，細胞増殖期とリンクして発現する場合と，生育環境下の異物に応じて一過的に発現する場合が観察される．

II. 排出システムの生理的意義

1. 抗菌薬および消毒薬耐性

排出システムの研究は，抗菌薬，消毒薬や抗菌性色素に対する細菌の耐性機構を解明する目的で始まった経緯から，病原性の有無とは別に，多くの細菌で研究され成果が蓄積されている．個々の排出システムがどのような耐性をもたらすかについては，ほかの総説[17]を参照されたい．

排出システムが抗菌性化合物を能動的に排出し，その

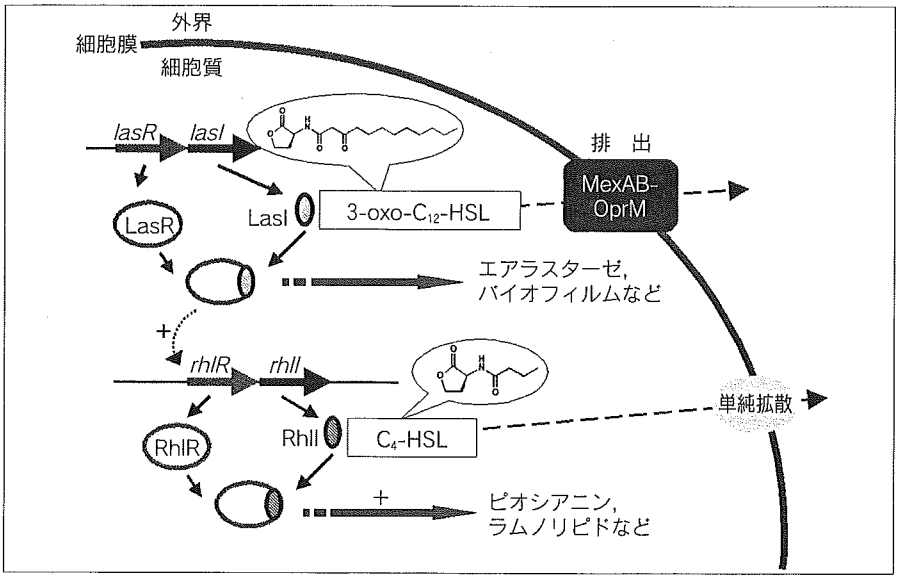

図 4　緑膿菌の細胞間コミュニケーションの作動と病原因子の産生
lasI 遺伝子産物によって合成された 3-オキソ-C_{12}-ホモセリンラクトン(3-oxo-C_{12}-HSL)は *lasR* 遺伝子産物と結合し，カスケード下流の *rhlR* 遺伝子と *rhlI* 遺伝子の発現を活性化する．3-オキソ-C_{12}-ホモセリンラクトンの細胞内蓄積はエラスターゼ，バイオフィルムなど，また，C_4-ホモセリンラクトン(C_4-HSL)の蓄積はピオシアニン，ラムノリピドなどの病原因子産生の引き金になる．3-オキソ-C_{12}-ホモセリンラクトンは MexA-MexB-OprM システムによって排出されてほかの細菌に取り込まれ，それが蓄積すると同じように病原因子産生が誘導される．

結果，抗菌性化合物の細胞内蓄積量が減少すること，作用標的への抗菌性化合物の到達量が減少することが耐性の原因である．さらに，排出システムによる抗菌性化合物耐性の特徴は基質域の広さにある．たとえば，緑膿菌によって排出される基質をみると，各種の抗菌薬，抗菌性色素，消毒薬にとどまらず，種々の有機溶媒や重金属までが排出される[3,4]．このような基質域の広さは排出システムを構成する蛋白質の構造に起因すると考えられる．その点については江田・中江の稿で論じられるのでここでは省略するが，排出される基質の分子内には疎水性官能基が存在することがひとつの共通点としてあげられる．また，これらの基質は細菌内で代謝されず，その蓄積と細胞障害が排出システム発現の引き金になっているのかもしれない．

2. 細菌間コミュニケーション機構と病原性への関与

抗菌薬耐性について多くの研究が蓄積されてきた排出システムではあるが，抗菌性化合物の排出が本来の生理的機能であるのかという疑問が長らく投げかけられてきた．それに答えるべく，排出システムの本来の機能を探る研究は多くの実験で試行錯誤されてきた．そしてこの答えは，緑膿菌のクオラムセンシング(quorum sensing)[→今月の Key Words (p.5)]や病原性との関連で明らかになってきた．クオラムセンシングはビブリオで発見された細菌間のシグナル伝達機構であるが，その主役は菌種特異的なアシルホモセリンラクトン誘導体であり，この化合物の細胞内への蓄積がクオラムセンシングの発動をひき起こす．多種の細菌でこの機構の研究が行なわれているが，病原性因子(エラスターゼ，ピオシアニン，ラムノリピド，ピオベルジン，遊走活性)の産生がこの機構と大きく関連していることが明らかになるにつれ，緑膿菌でもその研究はさかんになっている(**図 4**)．

Pearson ら[18]は，MexA-MexB-OprM システムが 3-オキソ-C_{12}-ホモセリンラクトンの排出に働くことを見いだした．そののち，MexA-MexB-OprM システム，MexC-MexD-OprJ システムや MexE-MexF-OprN システムの高発現は，クオラムセンシングに制御される病原因子の産生に影響し，マウスや線虫に対する緑膿菌の病原性を低下させることも報告されている．また，線虫，マウス，シロイヌナズナなどのモデル生物での緑膿菌の生存に必須の遺伝子の同定が行なわれたところ，排出システムを構成するコンポーネントの遺伝子がそれらのひとつとして同定されている[19]．さらに，MexH-MexI-OpmD システムの欠失はバナジウムを含む抗菌化合物に対する耐性を消失させるだけではなく，クオラムセンシングに制御される病原因子の産生を減少させることが報告された[16]．また，それらとは少し異なるが，マイクロアレイ実験によりクオラムセンシング依存的な遺伝子群を同定したところ，緑膿菌のいくつかの排出システムオペロンが見いだされた[20,21]．これらのことは，排出システムが細胞内で合成されたホモセリンラクトンの排出に働くことと，さらにはその発現もクオラムセンシングに制御されている可能性を示している．

一方，Hirakata ら[22]は，MexA-MexB-OprM システム

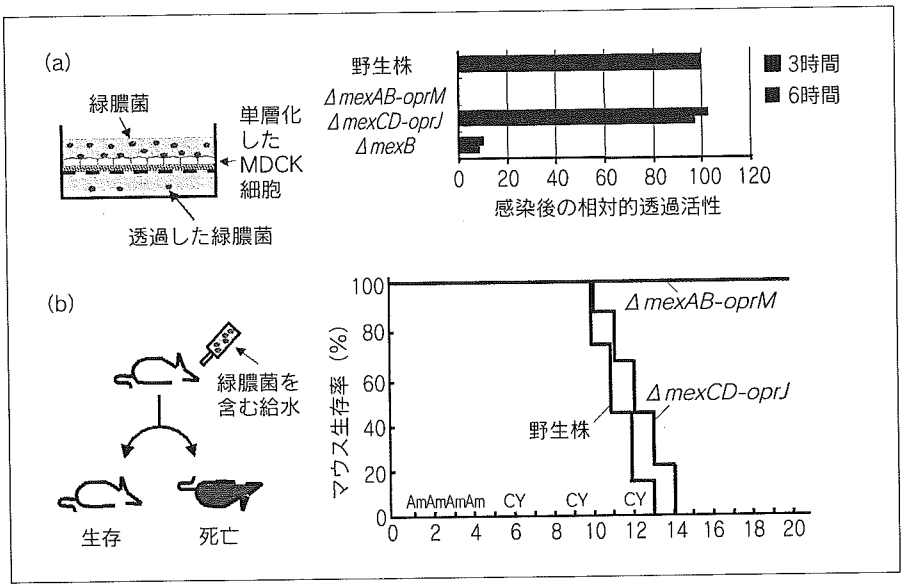

図5　緑膿菌のMDCK細胞単層の透過(a)と白血球減少マウスの致死効果(b)
(a)フィルター上に形成させたMDCK細胞単層を透過した緑膿菌の野生株細胞数は，*mexA-mexB-oprM* オペロンの欠失(Δ*mexA-mexB-oprM*)や *mexB* 遺伝子の欠失(Δ*mexB*)によって消失するが，別の排出システムをコードする *mexC-mexD-oprJ* オペロンの欠失(Δ*mexC-mexD-oprJ*)にはほとんど影響されない．(b)アンピシリン(Am)とシクロホスファミド(CY)の頻回投与によって白血球が減少したマウスに緑膿菌を混入させた飲料水を給水したところ，野生株でみられた13日目の全数致死効果が，*mexA-mexB-oprM* オペロンの欠失によって消失した．一方，*mexC-mexD-oprJ* オペロンの欠失は致死効果に影響を与えない．
[文献22より許可を得て転載]

の病原性への関与を調べた．フィルター上に形成させたMDCK細胞単層に対する緑膿菌の透過性を調べたところ，MexA-MexB-OprMシステムの欠失はMDCK細胞上皮への付着性を変化させることなく，侵入性を消失させることが見いだされた(図5a)．これは，緑膿菌感染症の病因のひとつである内因感染の消失を疑わせるものであり，この点を確かめるべく，白血球減少マウスを作製し緑膿菌浮遊液を飲料水として飲ませたところ，この欠失によってマウス致死効果が明らかに減少すること(図5b)，また，緑膿菌実験室株の培養上清を加えることによって，MexA-MexB-OprMシステムの欠失株で消失したMDCK細胞の単層透過性や白血球減少マウス致死効果が回復することを見いだした．しかし，MexA-MexB-OprM欠失株でのMDCK細胞単層透過性や白血球減少マウス致死効果の消失は3-オキソ-C_{12}-ホモセリンラクトンの添加によってはわずかにしか回復しないことから，この消失の原因はそれ以外の病原性発現に寄与する化合物の排出に関与しているものと考えられ，現在，その化合物の同定が行なわれている．

おわりに

抗菌薬や消毒薬に対する耐性機構研究のひとつとして，耐性の克服をめざし多くの研究が蓄積されてきた．しかしその一方で，抗菌薬や消毒薬といった，開発されて100年にも満たない化合物に対抗するために細菌に排出システムがあるとは考えられない．では，本来の生理的機能とは何かという疑問が長らく投げかけられてきた．研究の開始当初はそれに答えるべき研究方針を見いだすことはできなかったが，研究のなかで排出システムの驚くべき基質域の広さが明らかになるにつれて，排出システムの性状と機能の研究は拡大した．こうして，排出システムの本来の生理的機能のひとつが，細菌間のコミュニケーションに働くオートインデューサー化合物などの排出を介して細菌の病原性に関与することであると理解されるようになった．では，抗菌薬や消毒薬耐性は排出システムの副産物的機能なのだろうか？このシステムがそれらを排出するために進化の原初から用意されていたとは思えないが，抗菌薬も消毒薬も，いうなれば細菌にとって障害性異物であり，細胞内への侵入を阻止すべきものである．自然界には多種の障害性異物の存在が考えられ，それらに対して自己を防衛する機構は生物にとって必須であると考えられる．これは，さきにも述べたように，抗菌薬や細胞障害性異物の存在が排出システムの発現を誘導することからも支持されよう．

さらに，非病原性細菌である *Lactococcus lactis* のABC排出蛋白質LmrAをコードする遺伝子をヒト線維芽細胞で発現させたところ，ヒトのP糖蛋白質(MDR1)と同じように抗癌薬に対する多剤耐性化が起こり，また逆に，MDR1は大腸菌でもヒト細胞と同じ機能を発揮したと報告されている[23]．この事実は，同じ機能のABC排出蛋白質が生物界に広く保存されていることを示唆するものである．また，ヒト細胞リソソームでのコレステロール蓄積と細胞内コレステロールのホメオスタシスに

機能するNPC1蛋白質と緑膿菌のMexD排出蛋白質が，1次構造および2次構造において類似していることが示された[24]．これは，生物界に共通の排出蛋白質のホモログが広く保存され多種の機能を発揮していることや，排出蛋白質のプロトタイプが進化の出発点で存在したことを示し，さらには，細菌の排出システムの機能のひとつは，生育環境下に存在する細胞障害性異物の細胞内への進入阻止に働く自己防衛機構であるという考えと合致する．

本稿では，細菌のマルチコンポーネント型RND排出システムを例にして，排出システムの多様性とその機能について解説してきた．本稿で述べたように，抗菌薬耐性機構と病原性という，かつてはリンクするとは想像することもできなかったような領域が排出システムによって仲介されていることがわかった．排出システムが生物界に広く保存されていることから考えても，この研究は細菌の生理学的解明に重要なキーテーマである．

本稿で引用した筆者らの研究は，京都薬科大学微生物学教室のポスドク，大学院生，および卒論生の各氏の努力と，学外の研究施設(クイーンズ大学，ジュネーブ大学，東海大学医学部，長崎大学医学部，岡山大学薬学部，大阪大学産業科学研究所，三共(株)生物研究所)の多くの諸氏との共同研究によって推進されたものである．とくに，長崎大学医学部附属病院 検査医学教室の平潟洋一博士には，耐性機構研究に凝り固まっていた筆者の目を細菌病原性へと開いていただいたことを感謝します．

文 献

1) Koster, M., Bitter, W., Tommassen, J.：*Int. J. Med. Microbiol.*, **290**, 325-331 (2000)
2) Borges-Walmasley, M. I., Walmsley, A. R.：*Trends Microbiol.*, 9, 71-79 (2001)
3) Poole, K.：*Antimicrob. Agents Chemother.*, 44, 2233-2341 (2000)
4) Poole, K.：*Antimicrob. Agents Chemother.*, 44, 2595-2599 (2000)
5) Stover, C. K.：*Nature*, 406, 959-964 (2000)
6) Gotoh, N. *et al.*：*FEMS Microbiol. Lett.*, 165, 21-27 (1998)
7) Murata, T. *et al.*：*Biochem. Biophys. Res. Commun.*, 299, 247-251 (2002)
8) Nishino, K., Yamaguchi, A.：*J. Bacteriol.*, 183, 5803-5812 (2001)
9) Nishino, K. *et al.*：*Antimicrob. Agents Chemother.*, 47, 3030-3033 (2003)
10) Chuanchuen R., Narasaki C. T., Schweizer H. P.：*J. Bacteriol.*, 184, 5036-5044 (2002)
11) Cao, L., Srikmar, R., Poole, K.：*Mol. Microbiol.*, 53, 1423-1436 (2004)
12) Rouquette, C., Harmon, J. B., Sgafer, W. M.：*Mol. Microbiol.*, 33, 651-658 (1999)
13) Maseda, H. *et al.*：*FEMS Microbiol. Lett.*, 192, 107-112 (2000)
14) Morita, Y. *et al.*：*FEMS Microbiol. Lett.*, **202**, 139-143 (2002)
15) Masuda, N. *et al.*：*Antimicrob. Agents Chemother.*, 44, 2242-2246 (2000)
16) Aendekerk, S. *et al.*：*Microbiology*, 148, 2371-2381 (2002)
17) Pesci, E. C., Iglewski, B. H.：*Trends Microbiol.*, 5, 132-134 (1997)
18) Pearson, J. P. *et al.*：*J. Bacteriol.*, 181, 1203-1210 (1999)
19) Tan, M.-W. *et al.*：*Proc. Natl. Acad. Sci. USA*, 96, 2408-2413 (1999)
20) Schuster, M. *et al.*：*J. Bacteriol.*, 185, 2006-2079 (2003)
21) Wagner, V. E. *et al.*：*J. Bacteriol.*, 185, 2080-2095 (2003)
22) Hirakata, Y. *et al.*：*J. Exp. Med.*, 196, 109-118 (2002)
23) van Veen, H. W. *et al.*：*Nature*, 391, 291-295 (1998)
24) Davies, J. P. *et al.*：*Science*, 290, 2295-2298 (2000)

後藤直正
略歴：1978年 京都薬科大学大学院薬学研究科修士課程 修了，京都薬科大学 助手，講師，助教授を経て，2004年より京都薬科大学微生物学教室 教授．この間，信州大学医学部研究生，東海大学総合医学研究所 研究員，Cystic Fibrosis Foundation, Visiting Scientist． **研究テーマ**：細菌の排出システムと細胞間コミュニケーション機構，グラム陰性菌のゲノム配列解析と機能ゲノミクス．

ELSEVIER

FEMS Microbiology Letters 243 (2005) 125–131

FEMS MICROBIOLOGY Letters

www.fems-microbiology.org

Measurement of *Pseudomonas aeruginosa* multidrug efflux pumps by quantitative real-time polymerase chain reaction

Kazuhiko Yoneda [a], Hiroki Chikumi [a,*], Takeshi Murata [b], Naomasa Gotoh [b], Hiroyuki Yamamoto [a], Hiromitsu Fujiwara [c], Takeshi Nishino [b], Eiji Shimizu [a]

[a] *Division of Medical Oncology and Molecular Respirology, Department of Multidisciplinary Internal Medicine, Faculty of Medicine, Tottori University, 36-1 Nishi-machi, Yonago-shi, Tottori-ken 683-0805, Japan*

[b] *Department of Microbiology, Kyoto Pharmaceutical University, Yamashina, Kyoto 607-8414, Japan*

[c] *Department of Clinical Laboratory, Tottori University Hospital, 36-1 Nishi-machi, Yonago-shi, Tottori-ken 683-0805, Japan*

Received 21 October 2004; received in revised form 26 November 2004; accepted 29 November 2004

First published online 8 December 2004

Edited by A.M. George

Abstract

Multidrug efflux pumps contribute to multiple antibiotic resistance in *Pseudomonas aeruginosa*. Pump expression usually has been quantified by Western blotting. Quantitative real-time polymerase chain reaction has been developed to measure mRNA expression for genes of interest. Whether this method correlates with pump protein quantities is unclear. We devised a real-time PCR for mRNA expression of MexAB-OprM and MexXY-OprM multidrug efflux pumps. In laboratory strains differing in MexB and MexY expression and in several clinical isolates, protein and mRNA expression correlated well. Quantitative real-time PCR should be a useful alternative in quantitating expression of multidrug efflux pumps by *P. aeruginosa* isolates in clinical laboratories.

Keywords: *Pseudomonas aeruginosa*; Multidrug efflux pumps; Real-time polymerase chain reaction; Western blotting

1. Introduction

Pseudomonas aeruginosa is a clinically important pathogen showing greater intrinsic resistance than most other Gram-negative bacteria to a number of antimicrobial agents. This intrinsic resistance problem is compounded by increasingly frequent development of acquired resistance to agents that ordinarily show potent activity against this organism [1,2]. Thus *P. aeruginosa*, a major opportunistic pathogen, is becoming increasingly difficult to eradicate.

Several mechanisms are known by which this microorganism escapes the toxic effects of antimicrobial agents. These include production of inactivating enzymes, mutations of target enzymes, and multidrug efflux pumps [3–6]. The pumps, especially the resistance-nodulation-division (RND) family, have received particular recent attention because they can extrude multiple structurally unrelated compounds, and thus are involved in multidrug resistance [3,4,7]. To date, at least seven RND family drug efflux pumps are known to exist in *P. aeruginosa* cells. Among them, MexAB-OprM, which is expressed constitutively in wild-type strains, contributes to the intrinsic resistance of *P. aeruginosa* to most β-lactams and many other structurally unrelated antimicrobial agents [2,8,9]. MexXY-OprM also is involved in the intrinsic resistance of *P. aeruginosa* to several agents,

* Corresponding author. Tel.: +81 859 34 8105; fax: +81 859 34 8098.

E-mail address: chikumi@grape.med.tottori-u.ac.jp (H. Chikumi).

0378-1097/$22.00
doi:10.1016/j.femsle.2004.11.048

such as fourth-generation cephems, tetracyclines, erythromycin, and gentamicin [10,11]. Since expression of MexCD-OprJ and MexEF-OprN is strictly suppressed by the respective regulator genes in wild-type *P. aeruginosa* cells, neither of these efflux pumps are involved in intrinsic antibiotic resistance; they contribute only to acquired resistance [12,13].

An important part of investigating resistance mechanisms involving these efflux pumps in *P. aeruginosa* is determination of pump expression levels in laboratory strains or in clinical isolates. Conventionally, this has been done by Western blotting using monoclonal or polyclonal antibodies [1,2,9,14]. However, this method is complex and time-consuming, and the antibodies are not commercially available. A recently, developed new technique, quantitative real-time polymerase chain reaction (PCR), can measure mRNA expression for genes of interest. This method has proven highly accurate and reproducible in quantitating gene expression [15], and can quantify a given mRNA within a very large range of amounts [16]. However, the practicality of using this method to quantify gene expression of *P. aeruginosa* efflux pumps, as well as correlations of mRNA amounts with pump protein amounts, are uncertain. We set out to devise a real-time PCR as a sensitive, easily performed quantitative method for determining expression of two efflux pumps, MexAB-OprM and MexXY-OprM, that contribute to both intrinsic and acquired resistance. We considered this procedure as a possible alternative to quantification of pump proteins by Western blotting.

2. Materials and methods

2.1. Bacterial strains, media and growth conditions

The strains used in this study are shown in Table 1 [1,17,18]. *P. aeruginosa* clinical isolates were randomly selected from our collection at Tottori university hospital and Kyoto pharmaceutical university. Bacterial cells were grown in Luria–Bertani broth (LB) (Wako Pure Chemical Industries, Osaka, Japan). All bacterial cultures in LB were incubated at 37 °C with shaking (140 rpm) for 12.5 h.

2.2. Isolation of total membranes, SDS–PAGE, and immunoblot analysis

Cells grown in LB were harvested by centrifugation and total membranes were prepared as described previously [17]. Sodium dodecyl sulfate–polyacrylamide gel electrophoresis and electrophoretic transfer was performed as described previously [17]. The fractionated proteins were subjected to immunoblot analysis using anti-MexB rabbit-peptid antisera [17] or anti-MexY rabbit polyclonal antibody [32] as the primary antibodies and horseradish peroxidase-linked appropriate secondary antibodies (Pharmacia). The binding antibodies were detected using ECL plus Western blotting detection reagents (Amersham Pharmacia Biotech) according to the manufacture's instructions.

2.3. Cloning in plasmids and quantification of number of copies of the plasmids

Plasmids containing amplified sequences of PAO1 strain were constructed with the pGEM-T Easy Vector Systems (Promega, Tokyo, Japan) according to the manufacture's instructions. Briefly, the fragments of *mexB*, *mexY* and *rpsL* genes, 244, 246 and 241 bp, respectively, were amplified by conventional PCR with the primers listed in Table 2. The fragments were cloned into pGEM-T Easy Vector. DH5α *Escherichia coli* were transformed with these constructions, and after expansion in culture, the plasmids were purified by the Minipreps DNA Purification System (Promega). Gene

Table 1
Pseudomonas aeruginosa strains used in this study

Strain	Description	Source or reference
PAO1	Prototroph	
OCR1	MexAB-OprM-overproducing *nalB* mutant of PAO1	[7]
KG2212	Δ*mexR :: res*-Ω of PAO1	[17]
KG2239	Δ*mexR-mexA-mexB-OprM* of PAO1	[17]
KG5005	MexXY-overproducing, *nalB* Δ*mexAB* of PAO1	[18]
KG4545	*mexZ::*Ω Sm of PAO1	This study[a]
T-001	Clinical isolates	Kyoto Pharmaceutical University
T-002	Clinical isolates	Kyoto Pharmaceutical University
T-003	Clinical isolates	Tottori University
T-004	Clinical isolates	Tottori University
T-005	Clinical isolates	Tottori University
T-006	Clinical isolates	Tottori University
T-007	Clinical isolates	Tottori University
T-008	Clinical isolates	Tottori University
T-009	Clinical isolates	Tottori University

[a] KG4545 was constructed by insertion of Ω Sm cassette into the *mexZ* gene of PAO1 using allele exchange technique.

Table 2
Primers used in this study

Gene	Amplicon size (bp)	Sequences of primers
mexB	244	Forward: GTGTTCGGCTCGCAGTACTC Reverse: AACCGTCGGGATTGACCTTG
mexY	246	Forward: CCGCTACAACGGCTATCCCT Reverse: AGCGGGATCGACCAGCTTTC
rpsL	241	Forward: GCAACTATCAACCAGCTGGTG Forward: GCAACTATCAACCAGCTGGTG

quantification was performed with the BECKMAN DU-64 Spectrophotometer (Beckman Instruments, CA, USA) at a wavelength of 260 nm, and the number of copies was calculated. These plasmids were used as external standards. For each batch, serial plasmid dilutions were amplified; this allowed the construction of a standard curve and the quantification of mRNA in samples.

2.4. RNA extraction and cDNA synthesis

Total RNA was extracted from the 250 μl of cultured medium using QIAGEN RNeasy Mini Kit (Qiagen, Tokyo, Japan), and residual DNA was removed by adding DNase I using QIAGEN RNase-Free DNase Set (Qiagen) according to the manufacture's instructions. RNA was finally dissolved in 50 μl of RNase-free water. For cDNA synthesis, each 20 μl reaction contained 1 μg of total RNA, 10 μg of random hexamer, 1 × first strand buffer (50 mM Tris–HCl (pH 8.3), 75 mM KCl, 3 mM $MgCl_2$; Invitrogen, Tokyo, Japan), 0.5 mM dNTP, 10 U of RNase inhibitor (Invitrogen), and 200 U of Super Script II (Invitrogen). cDNA synthesis was performed in a TaKaRa PCR Thermal Cycler (Takara, Kyoto, Japan) according to the following procedure: after an annealing step for 10 min at 70 °C, reverse transcription was carried out for 50 min at 42 °C, followed by reverse transcriptase inactivation for 10 min at 95 °C.

2.5. Quantitative real-time PCR

The LightCycler (Roche, Tokyo, Japan) was used for all quantitative PCRs. All PCR amplification reactions were performed in a 10 μl volume containing a 3 mM concentration of $MgCl_2$, a 1 μM concentration of forward primers, a 1 μM concentration of reverse primers, 1 × FastStart DNA Master SYBR Green I (Roche), and 1 μl of diluted cDNA (1:10). The cycling parameters used were as follows: one denaturation cycle for 600 s at 95 °C and 45 amplification cycles (temperature transition rate of 20 $°C s^{-1}$) for 15 s at 95 °C, annealing for 5 s at 55 °C, extension for 10 s at 72 °C. Fluorescence readings were taken after each cycle following the extension step. This was followed by melting curve analysis of 65–99 °C (temperature transition rate of 0.1 $°C s^{-1}$) with continuous fluorescence readings. For each gene being measured, a sequence-specific standard curve was generated using 10-fold serial dilutions of plasmid DNA containing the sequence of interest and using the appropriate primers. The LightCycler software generated a standard curve from the standards and determined the gene copy number in each test sample. The ratios of gene expression between the target genes (*mexB*, *mexY*) and internal standard (*rpsL*) were expressed relative to those of PAO1 or KG4545, which is set at 1.00.

3. Results

3.1. Design of a real-time PCR assay for quantitative analysis of multidrug efflux pump

MexAB-OprM is considered the most important multidrug efflux pump in *P. aeruginosa*, being involved in broad resistance to cephems, penicillins, monobactams and carbapenems. We therefore first developed a quantitative real-time PCR assay targeted to *mexB* gene expression. Primer sequences were chosen from a region of the *mexB* gene that was preserved among the bacterial strains used in this study, according to DNA sequencing. In addition, an extensive search of several databases, including the EMBL and GenBank databases, indicated that no primer shared significant homology with other known nucleotides sequenced. To determine the copy number of *mexB* gene in sample, a standard curve was established with a control plasmid, pGEM-T/MexB, that contained the target *mexB* partial sequences. The control plasmid was diluted 10-fold with water in a serial manners, from 48 to 4.8×10^7 copies/μl, and each sample was submitted to the *mexB* real-time PCR (Fig. 1(a)). The threshold cycle number, which corresponds to the PCR cycle number at which the fluorescence signal exceeded the detection threshold, was plotted against each of logarithmically increasing standard DNA concentrations. As shown in Fig. 1(b), a linear relationship was obtained over on at least 7-log range of cDNA concentrations.

As MexXY-OprM is the other efflux pump system that contributes to intrinsic and acquired resistance to fourth-generation cephems and aminoglycoside derivative antibiotics, we similarly established a quantitative real-time PCR assay targeted to *mexY* gene expression. The range of quantification was from 88 to 8.8×10^7 copies/μl of pGEM-T/MexY construct (data not shown).

To compensate for varying numbers of cells in samples and efficiency of the reverse transcription reaction, we developed a quantitative real-time PCR reaction for *rpsL*, a constitutively expressed 30S rRNA gene,

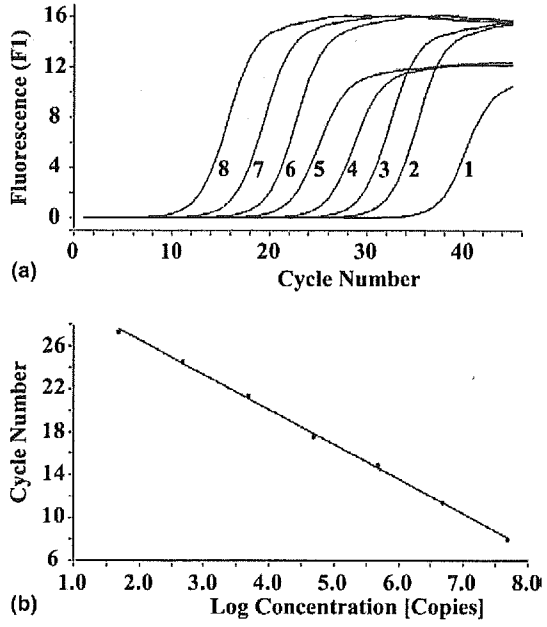

Fig. 1. Amplification profiles (a) and standard curves (b) for Light-Cycler PCR with SYBR Green I. (a) Performance of real-time PCR on a panel of control samples with predetermined numbers of copies of *P. aeruginosa* DNA. The plot shows the relationship of the fluorescent signal to cycle number in a panel of quantified copies of a plasmid containing the *mexB* fragment of a *P. aeruginosa* isolate. Samples: (1), water; (2), 48 copies/μl; (3), 480 copies/μl; (4), 4800 copies/μl; (5), 48,000 copies/μl; (6), 480,000 copies/μl; (7), 4,800,000 copies/μl; (8), 48,000,000 copies/μl. (b) Standard curve for real-time PCR. The threshold cycle number was plotted against each of the logarithmically increasing standard DNA concentrations for calibration.

for use as an internal standard [19]. The sequences of primers were based on previous the report which used them for conventional RT-PCR [20]. Quantitation proved to be linear over a wide logarithmical range, from 57 to 5.7×10^7 copies/l of pGEM-T/RpsL construct (data not shown).

3.2. Correlation between protein and mRNA expression of multidrug efflux pump in laboratory strains

We next used the real-time PCR assay to examine the correlation between protein and mRNA expression of MexB. For this purpose we used four laboratory strains, PAO1, OCR1, KG2212, and KG2239, that had been developed to express MexB to different degrees (Table 1). First we performed Western analysis to quantify protein expression of MexB in these bacterial strains (Fig. 2(a)). Densitometry of the MexB bands respectively showed protein expression in OCR1 and in KG2212 to be 2.9 and 1.3 times greater than in the control strain (PAO1), while no MexB band could be detected in KG2239 (Fig. 2(a)). Up- and down-regulation of MexB was investigated further by real-time PCR after culture under the same conditions. Expression of *mexB* mRNA in OCR1 and KG2212 respectively was 4 and 2.4 times greater than in PAO1, while only traces of *mexB* mRNA were found in KG2239 (Fig. 2(b)). Expression patterns of protein and mRNA thus were highly similar to one another in these laboratory strains.

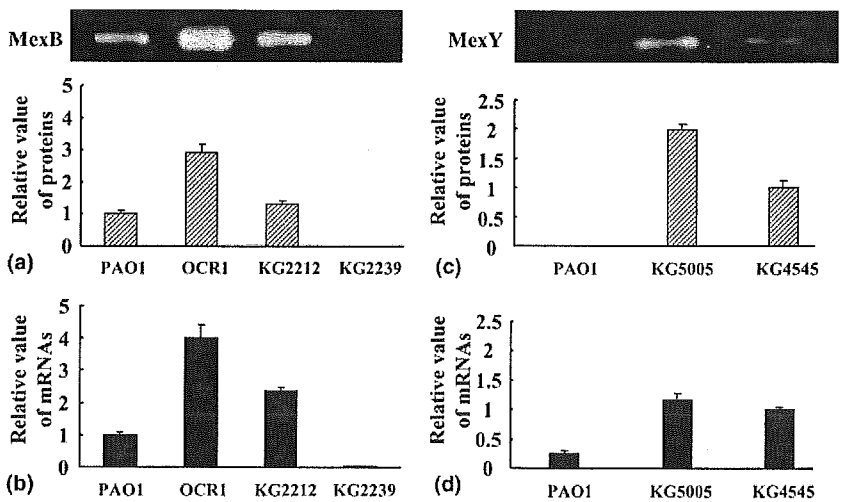

Fig. 2. Correlation between protein and mRNA expression of MexB and MexY in laboratory strains. (a) Western immunoblot analysis using a polyclonal antibody to MexB. Preparation of membranes (5 μg/lane) for immunoblot assay following SDS–PAGE was carried out as described in the Section 2 (upper panel). Band intensity was quantified using the Scion Image program based on the NIH Image for Macintosh program. Data are expressed relative to the quantity of MexB in PAO1. Each bar represents the mean ± SE of the relative intensity in three experiments (lower panel). (b) Quantitation of *mexB* gene expression by real-time PCR. Data are expressed relative to the quantity of *mexB* mRNA in PAO1. Each bar represents the mean ± SE of the relative intensity in three experiments. (c) Western immunoblot analysis using a polyclonal antibody to MexY. Preparation of membranes (5 μg/lane) for immunoblot assay following SDS–PAGE was carried out as described in Section 2 (upper panel). Band intensity was quantified using the Scion Image program based on the NIH Image for Macintosh program. Data are expressed relative to the quantity of MexY in KG4545. Each bar represents the mean ± SE of the relative intensity in three experiments (lower panel). (d) Quantitation of *mexY* gene expression by real-time PCR. Data are expressed relative to the quantity of *mexB* mRNA in KG4545. Each bar represents the mean ± SE of the relative intensity in three experiments.

Next we examined the correlation between protein and mRNA expression of MexY in three laboratory strains, PAO1, KG5005, and KG4545 (Table 1). Western analysis detected bands at 113 kDa representing the MexY protein in KG5005 and KG4545, while no band was seen in PAO1 (Fig. 2(c)). Quantification of the MexY bands showed high degrees of protein expression in KG5005 and KG4545, with expression of KG5005 being twice that of KG4545 (Fig. 2(c)). When expression of *mexY* was examined further by real-time PCR after culture under the same conditions, mRNA expression of *mexY* in KG5005 was 1.2 times that in KG4545, while expression in PAO1 was only 26% of that in KG4545 (Fig. 2(d)). These results were consistent with those of Western blotting.

3.3. Correlation between protein and mRNA expression of multidrug efflux pump in clinical isolates

Since laboratory strains chosen to vary in pump expression showed good correlations between protein and mRNA expression of both MexB and MexY, we next examined the relationship between protein and mRNA expression of MexB in randomly selected clinical isolates (T001 to T009; Table 1). As shown in Fig. 3(a), isolates T001, T002, T003, and T005 showed 1.6–2.3 times greater expression of MexB protein than did PAO1. On the other hand, T004 and T006 to T009, showed 50–100% lower expression than that in PAO1. Corresponding to this protein expression, mRNA expression measured by real-time PCR was higher than in PAO1 in T001, T002, and T003, but lower in T004 and T006 to T009 (Fig. 3(a)). The only exception was T005, which expressed 2.3 times as much protein as PAO1, but only slightly more mRNA.

Next, the same clinical isolates were examined concerning the relationship between protein and mRNA expression of MexY. By Western blotting, in T002 to T006, expression of MexY protein was equal to or greater than that in KG4545, while T001, T007, T008, and T009, like PAO1, did not express detectable MexY protein. In real-time PCR, T002 to T006 expressed more

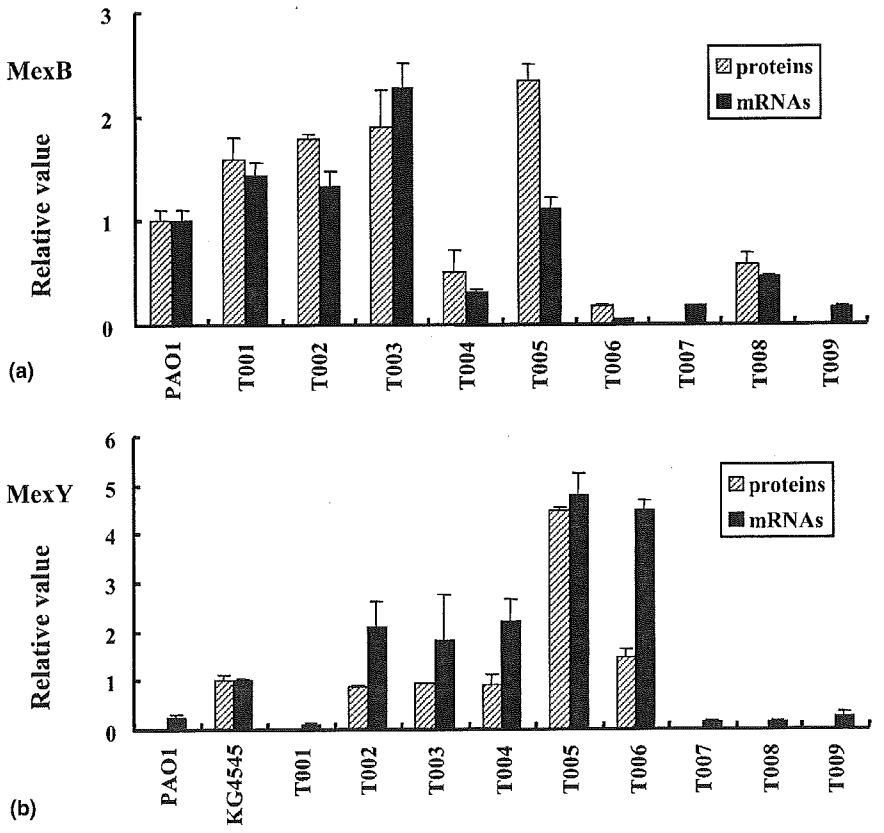

Fig. 3. Correlation between protein and mRNA expression of MexB and MexY in clinical isolates. (a) Hatched bars represent Western immunoblot analysis with a polyclonal antibody to MexB in clinical isolates. Band intensity was quantified using the Scion Image program based on the NIH Image for Macintosh program. Data are expressed relative to the quantity of MexB in PAO1. Each bar represents the mean ± SE of the relative intensity in three experiments. Solid bars represent quantitation of *mexB* gene expression by real-time PCR. Data are expressed relative to the quantity of *mexB* mRNA in PAO1. Each bar represents the mean ± SE of the relative intensity in three experiments. (b) Hatched bars represent Western immunoblot analysis with a polyclonal antibody to MexY in clinical isolates. Band intensity was quantified using the Scion Image program based on the NIH Image for Macintosh program. Data are expressed relative to the quantity of MexY in KG4545. Each bar represents the mean ± SE of the relative intensity in three experiments. Solid bars represent quantitation of *mexY* gene expression by real-time PCR. Data are expressed relative to the quantity of *mexY* mRNA in KG4545. Each bar represents the mean ± SE of the relative intensity in three experiments.

mexY mRNA than KG4545, while T001, T007, T008, and T009 as well as PAO1 expressed only very small amounts of *mexY* mRNA (Fig. 3(b)). Although amounts of protein were relatively small considering those of mRNA in T006, expression patterns of both mRNA and protein levels were quite similar in all other clinical strains. These data showed a general trend of increased protein resulting from increased mRNA.

4. Discussion

In this study we developed a quantitative real-time PCR assay to assess two multidrug efflux pumps in *P. aeruginosa*, MexB and MexY, and examined the relationship between mRNA expression measured by this real-time PCR and protein expression measured by Western blotting. Results obtained with our method, involving RNA isolation, cDNA synthesis, and quantitative real-time PCR, were highly reproducible and permitted precise quantification of minute or substantial amounts of *mexB* or *mexY* mRNA transcripts. Real-time PCR assay allowing quantification of efflux pump gene transcripts relative to those of the 30S rRNA gene, *rpsL*, showed good correlation with MexB and MexY protein expression in laboratory and clinical strains. This real-time PCR would appear to be a useful alternative method for assessing the multidrug efflux pumps MexB and MexY in *P. aeruginosa*.

Of the several techniques developed to estimate protein or mRNA expression, Western blotting is considered the "gold standard" for quantifying expression of multidrug efflux pumps in *P. aeruginosa*. Since this method is time-consuming and requires specific antibodies not commercially available, it has not been widely implemented in clinical laboratories. Real-time PCR has several practical advantages over Western analysis. First, real-time PCR has great sensitivity and a wide effective range. Even though the efflux pump proteins were not detectable in several of our strains, small amounts of corresponding mRNA could be detected and measured in all strains. Secondly, real-time PCR has high throughput and is less labor-intensive than Western analysis; it is a closed-tube system that does not require post-PCR handling. In our experience, total time for specimen processing and analysis is 3–4 h. Third, our application of real-time PCR has broad accessibility, being easy to perform in any laboratory with real-time PCR equipment as long as specific primers have been prepared. Therefore, real-time PCR is an attractive method for estimating gene expression for efflux pumps in bacteria.

As protein expression dose not always exactly reflect mRNA transcription, in case using mRNA expression profiles to presume the protein expression levels, we first needs to confirm the closeness of quantitative correlation of individual proteins with the corresponding mRNA. For example, while several reports have described good correlations between amounts of specific mRNA and corresponding protein expression [21,22], exhaustive studies of bacteria or fungi have reported no significant general correlation between protein and mRNA abundance [22–24]. As for multidrug efflux pumps in *P. aeruginosa*, the few previous studies estimating mRNA expression of these genes by conventional RT-PCR [25], or very recently by real-time PCR [19,26]. However, these works lacked the validation of a correlation between amounts of protein and mRNA expression. We therefore specifically examined this correlation, finding it to be significant for MexB and MexY in *P. aeruginosa*. Our results suggest that quantitative analysis of mRNA by real-time PCR might be a useful indicator of corresponding MexB and MexY protein quantities in lieu of Western blotting.

Although mRNA expression correlated well with protein expression levels in laboratory strains, some clinical isolates showed subtle discrepancies between protein and mRNA expression. Many molecular mechanisms causing these discrepancies have been reported to date. Such mechanisms include post-transcriptional control of the protein translation rate [27], the half-lives of specific proteins or mRNAs [28], and the molecular association of the protein products of expressed genes [29]. Clinical isolates have diverse genetic backgrounds, unlike laboratory strains that are isogenic with a reference strain such as PAO1. Heterogeneity in clinical isolates affects above regulatory mechanisms of transcription, translation, and proteolysis, leading to the discrepancies. In our study, all discrepancies shown in T005 or T006 appear likely to involve overall genetic heterogeneity of the strains, and therefore may be inevitable to some degree in clinical isolates.

In conclusion, real-time PCR based on the capillary format of the LightCycler instrument proved to be a simple, rapid, sensitive, and specific way to quantify multidrug efflux pumps in *P. aeruginosa*. Multidrug resistance of *P. aeruginosa* involves on interplay among multiple resistance mechanisms: β-lactamase, the outer membrane barrier, and multidrug efflux pumps [30,31]; optimal treatment will require a practical method for assessing the latter. Clinical laboratories should be able to estimate expression of these pumps by this method, permitting optimal choices involving antimicrobial agents, as well as antibiotics available for use with multidrug efflux pump inhibitors.

Acknowledgements

This research was partially supported by grants for scientific research to N.G. from the Ministry of Education, Culture, Sports, Science and Technology (MEXT)

of Japan and from the Ministry of Health, Labor and Welfare of Japan.

References

[1] Masuda, N. and Ohya, S. (1992) Cross-resistance to meropenem, cephems, and quinolones in *Pseudomonas aeruginosa*. Antimicrob. Agents Chemother. 36, 1847–1851.

[2] Poole, K., Krebes, K., McNally, C. and Neshat, S. (1993) Multiple antibiotic resistance in *Pseudomonas aeruginosa*: evidence for involvement of an efflux operon. J. Bacteriol. 175, 7363–7372.

[3] Nikaido, H. (2000) Crossing the envelope: how cephalosporins reach their targets. Clin. Microbiol. Infect. 6 (Suppl 3), 22–26.

[4] Hancock, R.E. and Brinkman, F.S. (2002) Function of *Pseudomonas* porins in uptake and efflux. Annu. Rev. Microbiol. 56, 17–38.

[5] Drlica, K. and Zhao, X. (1997) DNA gyrase, topoisomerase IV, and the 4-quinolones. Microbiol. Mol. Biol. Rev. 61, 377–392.

[6] Livermore, D.M. (1992) Interplay of impermeability and chromosomal β-lactamase activity in imipenem-resistant *Pseudomonas aeruginosa*. Antimicrob. Agents Chemother. 36, 2046–2048.

[7] Mine, T., Morita, Y., Kataoka, A., Mizushima, T. and Tsuchiya, T. (1999) Expression in *Escherichia coli* of a new multidrug efflux pump, MexXY, from *Pseudomonas aeruginosa*. Antimicrob. Agents Chemother. 43, 415–417.

[8] Gotoh, N., Tsujimoto, H., Poole, K., Yamagishi, J. and Nishino, T. (1995) The outer membrane protein OprM of *Pseudomonas aeruginosa* is encoded by *oprK* of the *mexA-mexB-oprK* multidrug resistance operon. Antimicrob. Agents Chemother. 39, 2567–2569.

[9] Li, X.Z., Nikaido, H. and Poole, K. (1995) Role of MexA-MexB-OprM in antibiotic efflux in *Pseudomonas aeruginosa*. Antimicrob. Agents Chemother. 39, 1948–1953.

[10] Masuda, N., Sakagawa, E., Ohya, S., Gotoh, N., Tsujimoto, H. and Nishino, T. (2000) Contribution of the MexX-MexY-oprM efflux system to intrinsic resistance in *Pseudomonas aeruginosa*. Antimicrob. Agents Chemother. 44, 2242–2246.

[11] Masuda, N., Sakagawa, E., Ohya, S., Gotoh, N., Tsujimoto, H. and Nishino, T. (2000) Substrate specificities of MexAB-OprM, MexCD-OprJ, and MexXY-oprM efflux pumps in *Pseudomonas aeruginosa*. Antimicrob. Agents Chemother. 44, 3322–3327.

[12] Kohler, T., Michea-Hamzehpour, M., Henze, U., Gotoh, N., Curty, L.K. and Pechere, J.C. (1997) Characterization of MexE-MexF-OprN, a positively regulated multidrug efflux system of *Pseudomonas aeruginosa*. Mol. Microbiol. 23, 345–354.

[13] Poole, K., Gotoh, N., Tsujimoto, H., Zhao, Q., Wada, A., Yamasaki, T., Neshat, S., Yamagishi, J., Li, X.Z. and Nishino, T. (1996) Overexpression of the *mexC-mexD-oprJ* efflux operon in *nfxB*-type multidrug-resistant strains of *Pseudomonas aeruginosa*. Mol. Microbiol. 21, 713–724.

[14] Srikumar, R., Li, X.Z. and Poole, K. (1997) Inner membrane efflux components are responsible for β-lactam specificity of multidrug efflux pumps in *Pseudomonas aeruginosa*. J. Bacteriol. 179, 7875–7881.

[15] Gibson, U.E., Heid, C.A. and Williams, P.M. (1996) A novel method for real time quantitative RT-PCR. Genome Res. 6, 995–1001.

[16] Heid, C.A., Stevens, J., Livak, K.J. and Williams, P.M. (1996) Real time quantitative PCR. Genome Res. 6, 986–994.

[17] Gotoh, N., Tsujimoto, H., Tsuda, M., Okamoto, K., Nomura, A., Wada, T., Nakahashi, M. and Nishino, T. (1998) Characterization of the MexC-MexD-OprJ multidrug efflux system in Δ *mexA-mexB-oprM* mutants of *Pseudomonas aeruginosa*. Antimicrob. Agents Chemother. 42, 1938–1943.

[18] Murata, T., Gotoh, N. and Nishino, T. (2002) Characterization of outer membrane efflux proteins OpmE, OpmD and OpmB of *Pseudomonas aeruginosa*: molecular cloning and development of specific antisera. FEMS Microbiol. Lett. 217, 57–63.

[19] Hocquet, D., Bertrand, X., Kohler, T., Talon, D. and Plesiat, P. (2003) Genetic and phenotypic variations of a resistant *Pseudomonas aeruginosa* epidemic clone. Antimicrob. Agents Chemother. 47, 1887–1894.

[20] Westbrock-Wadman, S., Sherman, D.R., Hickey, M.J., Coulter, S.N., Zhu, Y.Q., Warrener, P., Nguyen, L.Y., Shawar, R.M., Folger, K.R. and Stover, C.K. (1999) Characterization of a *Pseudomonas aeruginosa* efflux pump contributing to aminoglycoside impermeability. Antimicrob. Agents Chemother. 43, 2975–2983.

[21] Futcher, B., Latter, G.I., Monardo, P., McLaughlin, C.S. and Garrels, J.I. (1999) A sampling of the yeast proteome. Mol. Cell Biol. 19, 7357–7368.

[22] Washburn, M.P., Koller, A., Oshiro, G., Ulaszek, R.R., Plouffe, D., Deciu, C., Winzeler, E. and Yates 3rd, J.R. (2003) Protein pathway and complex clustering of correlated mRNA and protein expression analyses in *Saccharomyces cerevisiae*. Proc. Natl. Acad. Sci. USA 100, 3107–3112.

[23] Griffin, T.J., Gygi, S.P., Ideker, T., Rist, B., Eng, J., Hood, L. and Aebersold, R. (2002) Complementary profiling of gene expression at the transcriptome and proteome levels in *Saccharomyces cerevisiae*. Mol. Cell Proteomics 1, 323–333.

[24] Gygi, S.P., Rochon, Y., Franza, B.R. and Aebersold, R. (1999) Correlation between protein and mRNA abundance in yeast. Mol. Cell Biol. 19, 1720–1730.

[25] Evans, K., Adewoye, L. and Poole, K. (2001) MexR repressor of the *mexAB-oprM* multidrug efflux operon of *Pseudomonas aeruginosa*: identification of MexR binding sites in the *mexA-mexR* intergenic region. J. Bacteriol. 183, 807–812.

[26] Llanes, C., Hocquet, D., Vogne, C., Benali-Baitich, D., Neuwirth, C. and Plesiat, P. (2004) Clinical strains of *Pseudomonas aeruginosa* overproducing MexAB-OprM and MexXY efflux pumps simultaneously. Antimicrob. Agents Chemother. 48, 1797–1802.

[27] Nogueira, T. and Springer, M. (2000) Post-transcriptional control by global regulators of gene expression in bacteria. Curr. Opin. Microbiol. 3, 154–158.

[28] Varshavsky, A. (1996) The N-end rule: functions, mysteries, uses. Proc. Natl. Acad. Sci. USA 93, 12142–12149.

[29] Gerth, U., Kirstein, J., Mostertz, J., Waldminghaus, T., Miethke, M., Kock, H. and Hecker, M. (2004) Fine-tuning in regulation of Clp protein content in *Bacillus subtilis*. J. Bacteriol. 186, 179–191.

[30] Li, X.Z., Zhang, L. and Poole, K. (2000) Interplay between the MexA-MexB-OprM multidrug efflux system and the outer membrane barrier in the multiple antibiotic resistance of *Pseudomonas aeruginosa*. J. Antimicrob. Chemother. 45, 433–436.

[31] Okamoto, K., Gotoh, N. and Nishino, T. (2001) *Pseudomonas aeruginosa* reveals high intrinsic resistance to penem antibiotics: penem resistance mechanisms and their interplay. Antimicrob. Agents Chemother. 45, 1964–1971.

[32] Hocquet, D., Vogne, C., El Garch, F., Vejux, A., Gotoh, N., Lee, A., Lomovskaya, O. and Plesiat, P. (2003) MexXY-OprM efflux pump is necessary for a adaptive resistance of *Pseudomonas aeruginosa* to aminoglycosides. Antimicrob. Agents Chemother. 47, 1371–1375.